Grammage dependence of paper thickness

Grammage dependence of paper thickness

Jean-Francis Bloch[1], Merve Engin[2] and William W. Sampson[2,*]

[1]Université Grenoble Alpes, CNRS, Grenoble INP, 3SR Lab, F-38000 Grenoble, France
[2]School of Materials, University of Manchester, Manchester, M13 9PL, UK
*Corresponding author: w.sampson@manchester.ac.uk

Summary

We present a simple model for the nonlinear dependence of paper thickness on grammage and compare this to the results of a parallel experimental investigation using handsheets. From conventional measurements of grammage and thickness combined with X-ray microtomographic analysis, we demonstrate the influence of the structure of sheet surfaces on the porosity profile and hence on the sheet thickness. Further, we show that despite their higher porosity, the mean pore height in low grammage sheets is lower than that in the higher grammage sheets, implying that pore heights in surface layers are smaller than those in the bulk.

Keywords: Grammage, thickness, apparent density, porosity, modelling

Introduction

Whereas consumption of printing and writing grades of paper has decreased over recent years with the rise of digital technologies, paper remains among the most ubiquitous materials in society, with its use for packaging and hygiene grades increasing and predicted to continue to do so *(1, 2)*. In common with many materials systems, industrial and commercial drivers are for lighter weight paper products delivering the specified end-use performance. The mechanical, optical, and transport properties of paper, which form the basis of product specifications, are highly interdependent and strongly influenced by density. Overviews of these dependencies and of structure-property-process relationships are provided by, *e.g.*, Sampson *(3)* and Niskanen & Alava *(4)*.

Paper is a porous layered stochastic fibrous material: as a consequence of the continuous filtration process by which it is formed, the constituent cellulosic fibres lie essentially in the plane of the sheet *(5, 6)* and the voids between them exhibit a distribution of sizes *(7-9)*. In the plane of the network, the pore size has a gamma distribution with mean at least double the mean plane-perpendicular dimension or 'pore height' *(10)*, which exhibits an exponential distribution; we note that the exponential distribution is a special case of the gamma distribution. The pore size distribution in paper is important for filtration processes and barrier properties, and models for this property typically assume constant porosity in the thickness direction. Recent tomographic analysis of commercial and laboratory-formed papers reveal a near-symmetrical distribution of porosity, with surface layers being more porous than those in the bulk of the sheet, as anticipated for a rough near-planar porous material *(11,12)*.

The inherent in-plane heterogeneity of paper, coupled with its compressibility and surface roughness makes its mean thickness hard to define *(13,14)*. International standards specify the use of a dead-weight micrometer with a 16 mm circular diameter platen to measure the thickness of a single sheet or a stack of sheets under an applied pressure of 100 kPa (ISO 534:2011) or 50 kPa (TAPPI T411 om-97). Fellers *et al. (15)* note that such measures over-estimate thickness by an amount dependent on the relative magnitudes of surface roughness and total thickness. They recommended that for experimental investigations, sheets with a range of grammages are formed and their thickness, as determined from measurements on

single sheets, is plotted against grammage. The resultant plot exhibits a linear relationship with a positive intercept that represents the contribution of surface effects to thickness and the intrinsic thickness may be determined from the measured value minus that of the intercept; the intrinsic density is given by the reciprocal of the gradient of the plot. If samples with a range of grammages are not available, then density is typically reported as an apparent density, as given by the ratio of grammage to apparent thickness. For sheets of grammage less than about 80 g m^{-2}, this measure is strongly influenced by the contribution of sheet surfaces *(14)*.

Although the use of plots of thickness against grammage are valuable in supporting assumptions of constant density in experimental investigations of the mechanical behaviours of paper and other heterogeneous fibrous materials *(16-18)*, it is clear that if a full range of grammages is considered, then any plot of thickness against grammage must deviate from the linearity observed at higher grammages and pass through the origin. Inevitably, this has consequences for the density of the sheet at lower grammages and hence for the inter-fibre pore size distribution.

Here, an investigation is presented using standard grammage and thickness measurements along with computed X-ray tomography to probe the weight-dependence of thickness and hence that of porosity and pore size in laboratory made paper samples. We begin with development of a simple model for the porosity profile of the sheet, which provides insights into the observed experimental relationships between thickness and grammage.

Theory

Here, from consideration of the porosity profiles in the thickness direction shown by du Roscoat *et al. (11,12)*, a simple model for the porosity profile of paper is provided, and subsequently used to give the relationship between grammage and thickness. For simplicity, in the first instance sheet thickness, Z, is used as the free parameter; subsequently, a change of variables is used to provide expressions in terms of grammage, β.

Assumptions:

- the porosity profile of the sheet is symmetrical about its central plane;
- porosity in the surface region is a decreasing linear function of thickness;
- if the central plane is at a distance greater than t_s from the sheet surfaces, then the sheet exhibits a central bulk region with constant porosity, ε_b.

These assumptions give rise to the following expression for the porosity, ε, at a distance $0 \le z \le Z/2$ from a surface:

$$\varepsilon(z) = \begin{cases} 1 - \dfrac{z}{t_s}\left(1 - \varepsilon_b\right) & \text{for } 0 \le z \le t_s \\ \varepsilon_b & \text{for } t_s < z \le Z/2 \end{cases}, \qquad [1]$$

where Z is the sheet thickness.

Eq. 1 is plotted in Figure 1 for a structure with $Z > t_s$ such that a bulk region is present. Figure 2 shows the range of profiles captured by *Eq. 1*; on the top row (Figures 2a to 2c) $Z \le t_s$ and the structure consists only of surfaces—no bulk region is present. Figure 2d shows the initiation of the bulk region such that the mean porosity is surface-dominated. At high grammages, where $Z >> t_s$, the mean porosity is dominated by the bulk region, as shown in Figure 2f. Note that for sheets that exhibit a bulk region, the mean surface porosity is $(1 + \varepsilon_b)/2$.

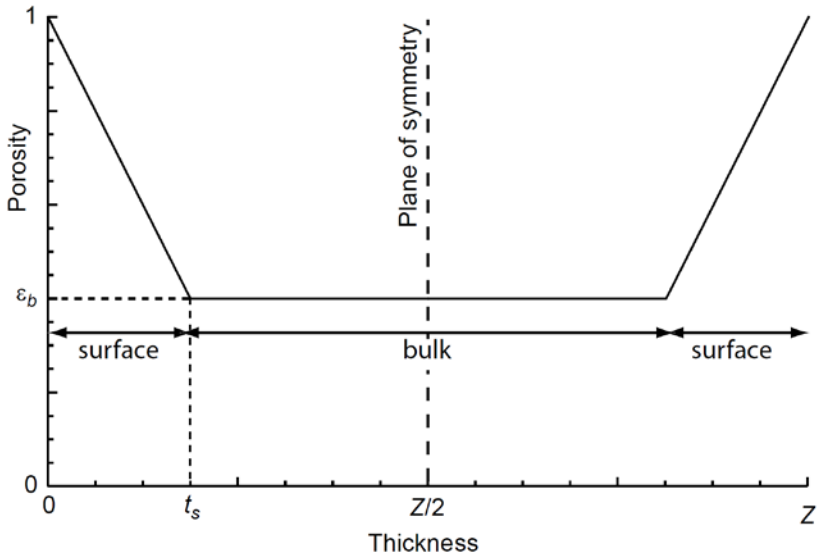

Fig 1. Example porosity profile as given by *Eq. 1* for a sheet with surface and bulk regions.

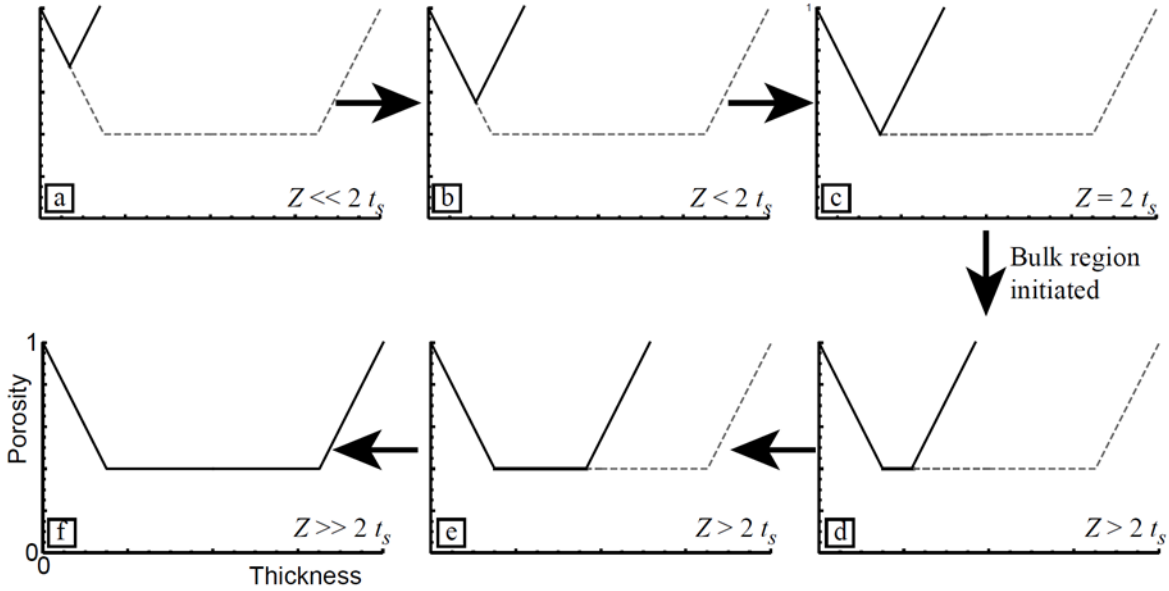

Fig. 2. Expected porosity profiles for sheets with increasing grammage, and hence thickness, as given by *Eq. 1*; solid lines show sheet profile, broken lines show full range predicted by model.

From *Eq. 1*, it follows that the mean porosity of a sheet with thickness, Z is given by

$$\bar{\varepsilon} = \frac{2}{Z}\int_0^{Z/2} \varepsilon \, \mathrm{d}z = \begin{cases} 1 - \dfrac{(1-\varepsilon_b)Z}{4t_s} & \text{for } 0 \le Z \le 2t_s \\ 1 - \dfrac{(Z-t_s)(1-\varepsilon_b)}{Z} & \text{otherwise.} \end{cases} \qquad [2]$$

Now, the apparent density of the sheet is given by

$$\rho = \frac{\beta}{Z} = (1-\bar{\varepsilon})\rho_c, \qquad [3]$$

where ρ_c is the density of the cellulosic fibre wall.

Table 1: Fibre morphologies

	Average fibre properties				
	Wetness (SR)	Length* (mm)	Width (μm)	Coarseness (μg m^{-1})	Fibre grammage (g m^{-2})
Spruce	20	2.6	21.6	155	7.2
	30	2.5	21.5	154	7.2
	45	2.4	21.7	155	7.1
Birch	20	0.90	12.4	53	4.3
	30	0.81	12.6	57	4.5
	45	0.76	12.6	55	4.4
Pine	12	2.2	20.8	141	6.8

*Length-weighted average fibre length

Substituting *Eq. 2* in *3* and solving for *Z* yields, on manipulation,

$$Z = \begin{cases} 2\sqrt{\dfrac{\beta t_s}{(1-\varepsilon_b)\rho_c}} & \text{for } 0 \le \beta < (1-\varepsilon_b)\rho_c t_s \\ t_s + \dfrac{\beta}{(1-\varepsilon_b)\rho_c} & \text{otherwise.} \end{cases} \quad [4]$$

For completeness, it should be noted that the analysis presented here does not distinguish between inter-fibre porosity and intra-fibre porosity since their contribution to the interdependence of grammage and thickness is the same.

Experimental

Experiments were carried out to test the theoretical relationships given by *Eqs. 1* and *4*. Once-dried commercial bleached Kraft pulps were selected for papermaking: spruce (Mercer International), pine (Stora Enso, Lapponia) and birch (Södra Gold). Pulps were soaked for 24-hours prior to being beaten in the Valley beater (TAPPI T-200 sp-01). For the spruce and birch, samples were taken at Schopper-Riegler wetnesses of (SR-) 20, 30, and 45; for the pine a light beating to SR-12 was carried out to remove any latent curl. All pulps were screened using a Somerville fractionator (TAPPI T-275 sp-02) fitted with an 80-mesh screen to remove all fines and smaller fibrous particles.

A British Standard Sheet Former was used to form handsheets from these 'fines-free' pulps with a range of grammages between 5 and 60 g m^{-2}. Given the fragile nature of the wet low-grammage sheets, a fine 6-end satin weave nylon fabric (warp: 36 yarns/cm; weft: 12 yarn/cm) was placed over the wire before forming to support the sheet during removal after couching. These fabrics remained in place for subsequent pressing between blotters, which was carried out at 1 MPa (150 psi), and during drying between blotters using a Japo MR-3D (Japo, Japan) laboratory dryer with drum temperature of 100°C. For consistency of process, these modifications to standards were applied for all sheets, regardless of grammage; all other aspects of sheet forming were carried out according to TAPPI Standard T-205 sp-02.

For the pine pulp, additional handsheets were made containing either 10% or 20% fines. Fines were obtained by beating the pulp in a Valley Beater for 180-minutes, fractionating with a 200-mesh and collecting the fraction that passed through the mesh on a clean muslin cloth. Following preliminary experiments to determine the relative retentions of fines and the fines free-fraction, sheets were formed from pulps with appropriate fines content to yield 10% or 20% in the final sheet. Full details of the experimental protocol are provided in *(17)*.

Table 2. Fitting data for Figure3.

		Fit to *Eq. 4*			Linear regression for $\beta > 20$ g m^{-2}		
		t_s (μm)	ε_b	β_s (g m^{-2})	Intrinsic density (g cm^{-3})	Intrinsic porosity	Intercept (μm)
Spruce	SR-20	19.4	0.581	12.6	0.683	0.545	25.9
	SR-30	18.4	0.582	11.9	0.674	0.551	23.9
	SR-45	18.7	0.566	12.6	0.689	0.541	22.8
Birch	SR-20	19.4	0.654	10.4	0.567	0.622	27.1
	SR-30	20.9	0.619	12.4	0.630	0.580	28.7
	SR-45	21.4	0.593	13.5	0.667	0.555	28.0
Pine	Fines-free	33.4	0.641	18.6	0.572	0.619	39.1
	10% fines	33.0	0.564	22.3	0.679	0.547	36.1
	20% fines	29.8	0.554	20.6	0.703	0.531	33.6

Fibre morphologies for all pulps, summarised in Table 1, were measured using a Metso FS5 Fibre Analyser (Valmet, Espoo, Finland). Measurements were repeated three times for each condition and the mean computed from measurements of over 5000 fibres (softwood) and over 10,000 fibres (hardwood). In each case reproducibility of the computed means was excellent and varied by less than 2% across the repeats. Grammage and thickness (TAPPI T-220 sp-01 & TAPPI T-411 om-97, respectively) of all samples were measured on sheets that had been conditioned for 24 hrs at 23 ± 1°C and 50 ± 2% RH immediately after drum drying.

X-ray microtomography was carried out on the LS/2343 ID19 beam-line at the European Synchrotron Radiation Facility (ESRF). Handsheets formed from the fines-free spruce pulp with original wetness SR-30 across the range of grammages made were selected for tomography, since the fibre dimensions were large relative to the system resolution of 0.65 μm/voxel. Samples were mounted on a capillary on a rotational stage using a *Post-it*® adhesive mounting, following the procedure described by du Roscoat *et al. (11,12)* and their methods for de-noising, global thresholding and binarising were followed. The volume imaged was 1.5 mm × 1.5 mm × sample thickness.

Tomographs were processed using *FIJI* image processing software. Raw files were saved as a stack of two-dimensional TIFF images and subsequently cropped to reduce file size. The z-directional porosity profile of a specimen was determined and measured target area of each layer was identified. Porosity was evaluated from the binarised data for each x-y layer as the ratio of the voxels belonging to the pore phase, to the total number of voxels in the volume. Pore heights were measured from x-z and y-z slices by counting the number of pixels representing voids between fibre surfaces; inevitably, the number of pore heights measured increased with the grammage of the sample, but was greater than 5000 in all cases.

Results and Discussion

Plots of thickness against grammage for each pulp are shown in Figure 3. In each plot the broken lines represent a least squares fit of *Eq. 4* to the data. The free parameters for fitting, t_s and ε_b, are given in Table 2 along with the threshold grammage at which the bulk region is initiated, computed as $\beta_s = (1-\varepsilon_b)\rho_c t_s$; given our assumption of symmetry, we note that the grammage in each surface is $\beta_s/2$. Here and throughout, we have assumed ρ_c = 1.5 g.cm^{-3}. Although the cell wall density will be somewhat reduced by moisture content, simple analysis shows that a typical moisture content of 7% would result in less than 3% relative error in our

a)

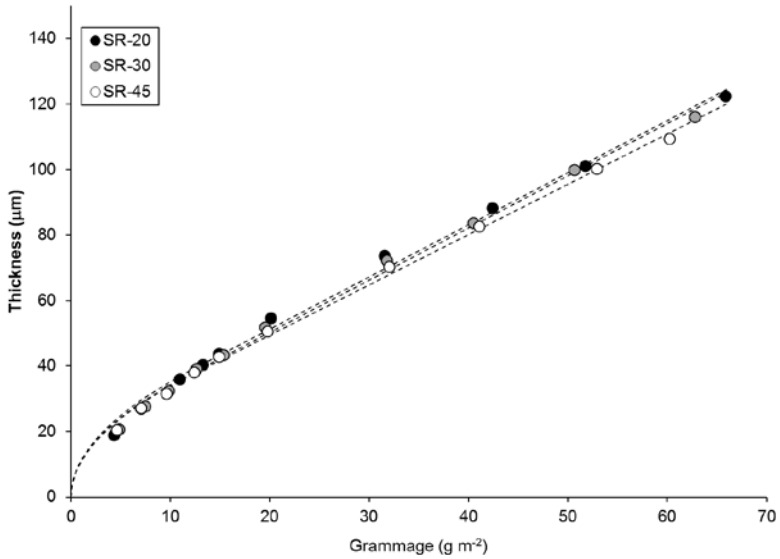

b)

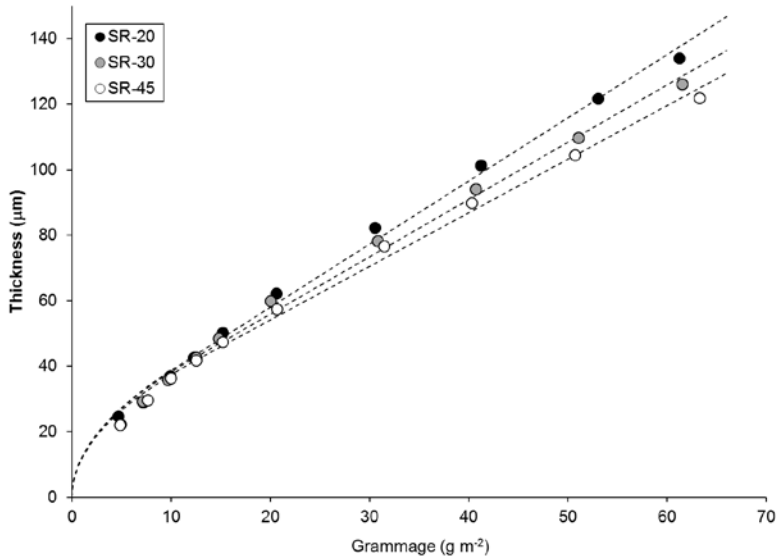

c)

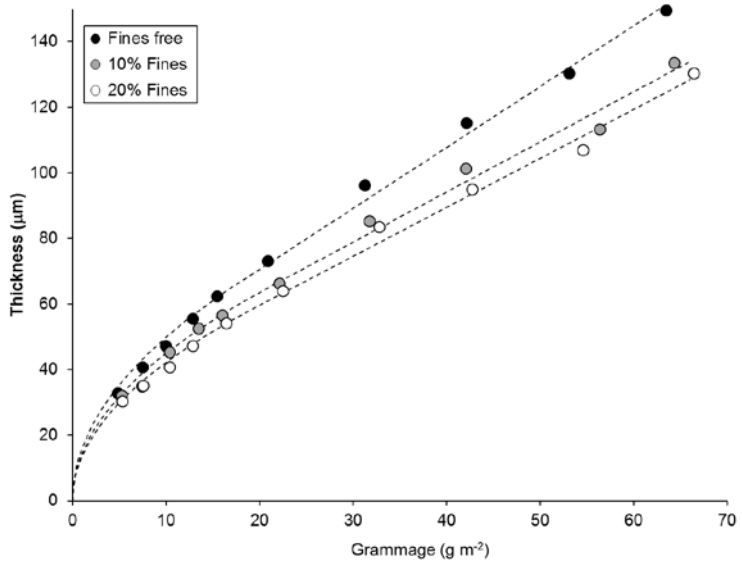

Fig. 3. Thickness against grammage for handsheets formed from a) fines-free spruce pulps, b) fines-free birch pulps, c) pine pulps with controlled fines contents. Broken lines represent least-squares fit of *Eq. 4* to the data; regression data are given in Table 2

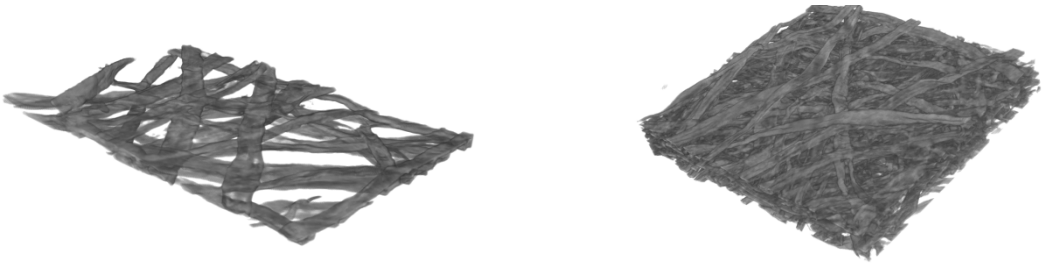

Fig 4: Tomographic reconstructions of spruce handsheets. Left: 7.5 g m^{-2}; right: 60 g m^{-2}

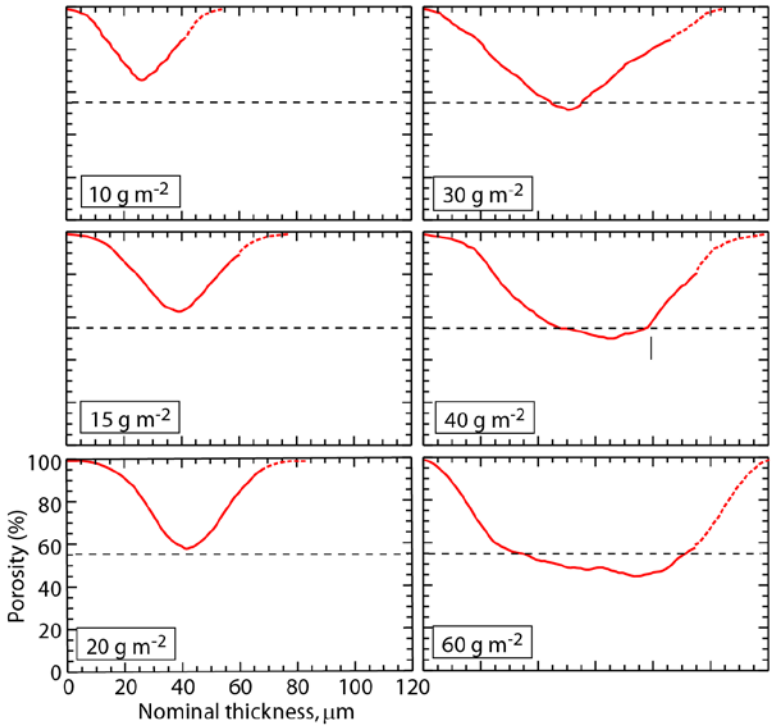

Fig. 5. Porosity profiles obtained via X-ray microtomography for spruce handsheets of different grammages. The scales on the bottom left apply to all plots.

estimate of porosity; similarly, the influence of hemicellulose content on cell wall density can be considered negligible. The coefficient of determination, r^2, was computed for each curve fit and in all cases these were greater than 0.98. In all cases, the model slightly overestimates the experimental data at the lowest grammages, though for all data the greatest residual is less than 4 µm. Given the simplicity of our model, and the accuracy of measurements, agreement is very good.

For completeness, a linear regression was carried out on the data in Figure 3 for grammages greater than 20 g m^{-2} and the reciprocal of the gradient taken to yield the intrinsic density, as recommended by Fellers *et al. (15)*; the intrinsic porosity computed from these is reported in Table 2 also; in all cases these linear regressions gave, $r^2 > 0.97$ and we observe that for a given pulp the intercept from these linear regressions can be considered constant. It is interesting to note the insensitivity of the intrinsic density of the fines-free softwood pulps to beating, which is consistent with the importance of Kraft fines to sheet consolidation reported by Sirviö and Nurminen *(19)*.

We selected the sheets formed from fines-free spruce pulp with original wetness SR-30 for X-ray microtomographic analysis, as described above. The porosity of 1-voxel layers in the plane of the sheet was computed from the binarised image starting at the free surface; the

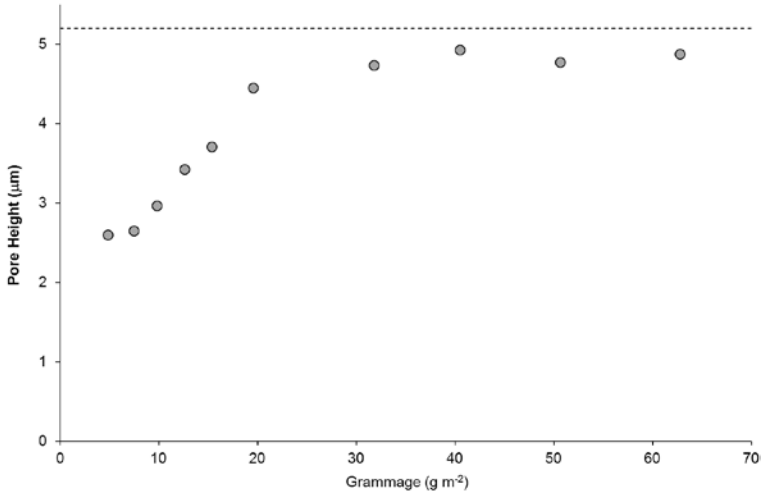

Fig. 6. Mean pore heights as measured from tomographs plotted against grammage for sheets formed form spruce pulp

analysis stopped when adhesive from the *Post-it*® was identified. Examples of reconstructed network structures are shown in Figure 4 and the resultant porosity profiles are shown in Figure 5. For each profile, the top surface was defined as the first slice with porosity less than 99%, accordingly, the horizontal axis is labelled 'nominal' thickness, since the thickness obtained using standard laboratory methods is likely to start at some lower porosity; it should be noted however that the spatial calibration applied, using the resolution of the voxel, gives faithful units of µm, such that gradients are meaningful.

To aid intuitive interpretation of the profiles in Figure 5, data from the top surface has been reflected in a vertical line at the centre of the profile as an assumed representation of a symmetrical bottom surface; this is shown as a broken line in each profile. As might be anticipated, sheets with grammages below 10 g m^{-2} were somewhat fragile to handle and tended to exhibit some partially detached fibre ends, which gave raise to artefacts in the tomographs. As such, these are excluded from our analysis. The broken horizontal lines in Figure 5 represent the intrinsic porosity of the sample, calculated as given in Table 2.

The qualitative agreement between the measured porosity profiles in Figure 5 and those predicted by our theory, as shown in Figure 2, is immediately apparent. For grammages of 20 g m^{-2} or lower, the porosity profiles in Figure 5 exhibit sharp minima and remain above the intrinsic porosity. At higher grammages, the minimum in the profile occurs within a central region of approximately constant porosity, marginally less than ε_{int}, and this represents the network bulk.

Now, the porosity in the surface regions includes voids between vertically adjacent fibres, and surface pores that are unbounded. From our theoretical treatment, we have shown that we can use thin sheets to represent surface regions of thicker sheets. In sheets with low grammage, and hence in the surface layers, we expect vertical separation between fibres to be rare, whereas at higher grammages, porosity is dominated by the bulk region, and vertical separation between fibres defines the porous structure of the sheet. Figure 6 shows the mean 'pore height' calculated from our tomographs as the distance between adjacent fibre surfaces in the z-direction. Sampson *(20)* gives the mean pore height for isotropic fibrous structures, *i.e.* those without the surface porosity gradients identified here, as

$$\overline{h} = \frac{\varepsilon}{1-\varepsilon} t \qquad [5]$$

where t is fibre thickness. The broken horizontal line in Figure 6 represents the mean pore height calculated using *Eq. 5* using the mean porosity of the bulk region identified in Figure 5 ($\varepsilon = \varepsilon_b = 0.52$) and assuming the fibre thickness to be given by the fibre grammage divided by the density of cellulose (t = 4.8 μm) *(21)*.

It is illustrative to consider the data in Figure 6 along with the profiles shown in Figure 5. From Figure 6, we make the counter-intuitive observation that at low grammages, the mean pore height increases steadily, whereas from Figure 5 we see a decrease in porosity. This arises from an increase in the incidence and size of vertical separation between adjacent fibre surfaces, which is coupled with a decrease in the fraction of the porosity that is unbounded at the sheet surfaces. Above around 20 g m^{-2}, the data in Figure 6 converge towards the value calculated for the bulk. Inevitably, given the contribution of smaller pore heights in the surfaces, which are implied by the data for lower grammages, the mean pore height at these higher grammages remains fractionally lower than that calculated for the bulk. Finally, we remark that an inevitable consequence of the pore height being lower at the surfaces, despite the porosity being higher, is that the mean in-plane pore size is greater at the surface than in the bulk.

Conclusions

A simple model for the porosity profile in paper, which takes account of the greater porosity of surface regions when compared to the bulk, has been presented. The model predicts a non-linear relationship between sheet grammage and thickness at lower grammages tending to an approximately linear dependence at higher grammages as the influence of surface layers decreases relative to that of the bulk. Comparison of the model with experimental data from X-ray microtomography of handsheets shows excellent qualitative agreement. Further comparison of the model using least-squares fitting to experimental data giving the relationship between grammage and thickness for handsheets shows very good agreement and provides a simple and low-cost method to estimate the contributions of surfaces to the thickness, and hence density, of handsheets. Finally, the tomographic analysis has been used to provide insights into the evolution of the pore height distribution with grammage.

References

(1) P. Haggett. Digital print developments and what it means of paper. *Appita J.* **71**(1): 14-15, 2018

(2) Global forest, paper and packaging survey: 2016 edition. PricewaterhouseCoopers, London, 2016

(3) W.W. Sampson, Materials properties of paper as influenced by its fibrous architecture, *Int. Mater. Rev.* **54**(3):134-156, 2009

(4) M. Alava and K. Niskanen, The physics of paper, *Rep. Prog. Phys.***69**(3):669-723, 2006

(5) B. Radvan, C.T.J. Dodson and C.G. Skold. Detection and cause of the layered structure of paper. In Consolidation of the Paper Web (F. Bolam, ed.), *Trans. IIIrd Fund. Res. Symp*., pp189-215. BPBMA, London, 1966

(6) D.W. Vahey and J. Considine. Tests for z-direction fibre orientation in paper. *Appita J.* **63**(1):27-31, 41, 2010

(7) W.C. Bliesner. A study of the porous structure of fibrous sheets using permeability techniques. *Tappi J*. **47(**7):392-400, 1964

(8) C.T.J. Dodson, A.G. Handley, Y. Oba and W.W. Sampson. The pore radius distribution in paper. Part I: The effect of formation and grammage. *Appita J.* **56**(4):275-280, 2003

(9) S. Roberts and W.W. Sampson. The pore radius distribution in paper. Part II: The effect of laboratory beating. *Appita J.* **56**(4):281-283,289, 2003

(10) W.W. Sampson and S.J. Urquhart. The contribution of out-of-plane pore dimensions to the pore size distribution of paper and stochastic fibrous materials. *J. Porous Mater.* **15**(4):411-417, 2008

(11) J.-F. Bloch and S. Rolland du Roscoat. Three-dimensional structural analysis. In Advances in Pulp and Paper Research, Oxford 2009 (S.J. I'Anson, ed.), *Trans. XIVth Fund. Res. Symp*., pp599-664, FRC, Manchester, 2009

(12) S. Rolland du Roscoat, M. Decain, X. Thibault, C. Geindreau, J.-F. Bloch. Estimation of microstructural properties from synchrotron X-ray microtomography and determination of the REV in paper materials. *Acta Mater.* **55**(8):2841-2850, 2007

(13) C.T.J. Dodson, Y. Oba and W.W. Sampson. On the distributions of mass, thickness and density in paper. *Appita J.* **54**(4):385-389, 2001

(14) Y.J Sung, C.H. Ham, O. Kwon, H.L. Lee, D.S. Keller. Applications of thickness and apparent density mapping by laser profilometry. In Advances in Paper Science and Technology (S.J. I'Anson, ed.), *Trans. XIIIrd Fund. Res. Symp*., pp961-1007. FRC, Manchester, 2005

(15) C. Fellers, H. Andersson and H. Hollmark. The definition and measurement of thickness and density. Ch. 7 in **Paper Structure and Properties** (J.A. Bristow and P. Kolseth, eds.), Marcel Dekker, New York, 1986

(16) S.J. I'Anson and W.W. Sampson. Competing Weibull and stress-transfer influences on the specific tensile strength of a bonded fibrous network. *Compos. Sci. Tech.* **67**(7):1650-1658, 2007

(17) W.W. Sampson and J. Yamamoto. The influence of fines, fibre contact and grammage on the free shrinkage of handsheets. *Appita J.* **64**(1):76-82, 2011

(18) V.A. Ramirez, P.J. Hogg and W.W. Sampson. The influence of the nonwoven veil architectures on interlaminar fracture toughness of interleaved composites. *Compos. Sci. Tech.* **110**(7):103-110, 2015

(19) J. Sirviö and I. Nurminen. Systematic changes in paper properties caused by fines. *Pulp Pap. Can.* **105**(8):T193-T196, 2004

(20) W.W. Sampson. **Modelling Stochastic Fibrous Materials with *Mathematica*®**. Springer-Verlag, London, 2009

(21) O.J. Kallmes and G.A. Bernier. Estimating the thickness of pulped wood fibres. *Nature* **197**:1330, 1963